AIAA AVIATION Forum
June 25-29, 2018, Atlanta, Georgia
2018 Aviation Technology, Integration, and Operations Conference

10.2514/6.2018-3045

Check for updates

Integrated Trajectory-Location-Routing for Rapid Humanitarian Deliveries using Unmanned Aerial Vehicles

Jose Javier Escribano Macias*, Dr Panagiotis Angeloudis † and Professor Washington Ochieng ‡
Imperial College London, London SW7 2BU, United Kingdom

Unmanned Aerial Vehicles have the potential to provide an economical solution to the challenges of post-disaster land-based relief operations. Beyond regulatory concerns, technical and particularly airspace integration limitations inhibit their deployment in practice. To address these issues and ensure uninterrupted optimal operations, we present a novel approach consisting of an integrated trajectory-location-routing algorithm that seeks to determine the optimal location of supporting infrastructure in the distribution supply chain. Unique to this approach is the consideration of dynamic obstacle avoidance and variable battery consumption relationships. An approximate algorithm based on a bi-level Large Neighbourhood Search is used to obtain close to optimal solutions under reasonable runtime. Results show that fleets of small UAVs could quickly distribute relief supplies to affected population groups with minimal reliance on ground infrastructure.

I. Nomenclature

Indices

i, j	=	nodes in network
t	=	mission time step
v	=	vehicles (UAVs)
e	=	element
o	=	obstacle

Sets

$\mathcal{N}$	=	nodes in Network
$\mathcal{H}$	=	hubs in network
$\mathcal{T}$	=	mission time horizon
$\mathcal{V}$	=	vehicle set
$\mathcal{E}$	=	elements in trajectory
$\mathcal{O}$	=	obstacle set

Aerodynamic Parameters

K	=	drag polar $[-]$
ρ	=	air density $[kilograms/metre^3]$
S	=	wind area $[m^2]$
$\Delta e_{i,j,t,e}$	=	flight time in element e of trajectory between nodes i and j initiated at t $[seconds]$
C_{D0}	=	parasite drag coefficient $[-]$

Control Variables

$\mathcal{T}$	=	thrust force $[Newtons]$
Ψ	=	heading angle $[radians]$
γ	=	flight path angle $[rads]$
$\mathcal{V}$	=	vehicle set

Force Parameters

$D_{i,j,t,e}$	=	drag force $[N]$
$L_{i,j,t,e}$	=	lift force $[N]$
W	=	weight $[N]$
m	=	mass $[kg]$
g	=	acceleration due to gravity $[m/s^2]$
a	=	vehicle acceleration $[m/s^2]$

Battery Parameters

P	=	power $[Watts]$
I	=	current $[Amps]$
V	=	voltage $[Volts]$
B	=	battery capacity $[AmpsHour]$
Δt	=	time step $[s]$
μ	=	battery efficiency $[-]$

State Variables

$U_{i,j,t,e}$	=	airspeed $[m/s]$

Routing Parameters

F	=	fixed setup costs of a hub [$]

*PhD Candidate, Department of Civil and Environmental Engineering, jose.escribano-macias11@imperial.ac.uk.
†Senior Lecturer in Engineering Systems and Logistics, Department of Civil and Environmental Engineering, p.angeloudis@imperial.ac.uk.
‡Chair in Positioning and Navigation Systems and Head of the Centre for Transport Studies, Department of Civil and Environmental Engineering, w.ochieng@imperial.ac.uk.

$SOC_{i,j,t,e}$ = State of Charge $[-]$
$x, y, z_{i,j,t,e}$ = Cartesian coordinates $[km]$
$C_{L_{i,j,t,e}}$ = lift coefficient $[-]$
$C_{D_{i,j,t,e}}$ = drag coefficient $[-]$
$\Delta e_{i,j,t,e}$ = flight time in element e $[s]$
σ = variable hub cost [$]
Pen = non-delivery penalty $[Amps]$
Q = vehicle payload capacity $[kg]$
C = time cost between nodes i and j [$]
A_i = aid demand at node i, a negative demand indicates supply $[kg]$
$\Delta t_{i,j,t}$ = flight time between nodes i and j at time t $[s]$
R_{xy}, R_z = horizontal and vertical safety distance $[km]$

Decision Variables
$r_{i,j,v,t}$ = Boolean determining if vehicle v travels from i to j at time t
$c_{i,j,v,t}$ = amount of cargo carried from i to j by vehicle v at time t
h_i = Boolean determining whether node i is a hub
u_i = unfulfilled demand to node i
s_i = slack variable for unfulfilled demand to node i
p_i = slack variable for unfulfilled demand to node i

II. Introduction

The field of humanitarian logistics aims to save lives in immediate peril through the rapid distribution of relief resources. With the frequency of natural hazards increasing due to climate change [1], the humanitarian community has initiated efforts to expand their operational capacity. As a result, expenditure has increased: the World Food Programme (WFP) Aviation Division has reported a 70% increment between 2011 and 2015 [2, 3], amounting to US$5,367 million for the WFP in 2016 [4]. In addition, the rapidly decreasing survival rate in disaster-impacted regions calls for the development of agile humanitarian response mechanisms [5].

Damage to infrastructure and inaccessibility to fuel further inhibits operational timelines, even when limited to aerial transport [6, 7]. Given the prohibitive level of expenditure required to expand the scale of existing operations, it is vital that respondents have access to efficient systems that minimise risk and cost. To this end, humanitarian organisations are seeking for alternative transport solutions that reduce capital investment and provide an agile response.

Given the recent advances in technology, the use of Unmanned Aerial Vehicles (UAVs) is increasingly being considered within the humanitarian community for logistics purposes [8]. Despite the several initiatives announced by both commercial and governmental organisations [9–14], major concerns hinder UAV integration into logistics sectors. Apart from the technical limitations relating to payload and range, several regulatory barriers remain. Currently, the National Aeronautics and Space Administration (NASA) and the European Aviation Safety Agency (EASA) are developing traffic management frameworks for low altitude UAVs in the form of Unmanned Aerial System Traffic Management (UTM) and U-Space respectively [15, 16]. Under both frameworks, UAVs will share airspace with other aircraft, with avoidance manoeuvering responsibilities residing on the operators. This calls for the development of integrated trajectory and routing modelling frameworks that consider the unique capabilities related to UAVs. Currently, UAV-based logistics models are formulated as Vehicle Routing Problems (VRP), which allow multiple features to be explored including multi-depot activities, fleet constraints, and budget limitations among others. Murray & Chu [17] formulate a variation of the Travelling Salesman Problem (TSP), where a conventional ground vehicle acts as a mobile depot for UAV deliveries to customers along its route. Nedjati et al. [18] evaluate UAV deployments for relief distribution using an integer programming approach. Coelho et al. [19] present a UAV-specific formulation of the Green Vehicle Routing Problem (G-VRP), that considers refuelling and recharging requirements for a fleet of UAVs with limited range. Dorling et al. [20] study urban goods distribution considering some aspects of energy use, but focused on multi-rotor vehicle operations and ignored field recharging.

The literature above does not consider tactical decisions (such as warehouse locations) that are necessary for humanitarian response and the deployment of extensive UAV operations. The Location-Routing Problem (LRP) incorporates these by introducing a bi-layer heuristic, overcoming scalability limitations of exact solutions [21, 22]. Sarıçiçek & Akkus [23] focused on UAV patrol problems using a homogeneous UAV fleet. Fikar [24] developed a decision support system for warehouse location and vehicle routing using a mixed fleet of ground and aerial vehicles. Mourelo et al. [25] proposed a bi-stage location-routing algorithm for truck-drone deliveries using a k-means location and genetic algorithm. Kim et al. [26] formulate a Mixed Integer Linear Problem (MILP) to find the optimal location and routing of drones for health-care services in rural areas.

The reviewed literature disregards path planning in their methodology, which facilitates accurate battery consumption calculation and conflict avoidance. As an initial step to integrate path planning and routing, Forsmo [27] introduces a model based on the TSP for optimal UAV path planning using multiple waypoints. Kim et al. [28] formulate a task scheduling algorithm partitioning each trajectory to allow UAVs to change the destination for recharge. Manyam et al. [29] present a multi-depot multi-vehicle TSP that considers motion constraints. Matthew et al. [30] develop a TSP for task scheduling and path planning in package delivery using a heterogeneous vehicle fleet. Finally, Furini et al. [31] present two time-dependent TSP models for controlled airspace operations, where conflict zones enforce minimum separation rules. All studies use Mixed Integer Linear (MILP) formulations and fail to capture nonlinear aerodynamic effects that emerge during flight. With the exception of the work carried out by Furini et al. [31], airspace management and collision avoidance have not been considered elsewhere in the reviewed literature.

Trajectory optimisation models are considered by a separate stream of research and have the potential to overcome such limitations. However, they lack scalability necessary for trajectory improvement and re-planning. Among sampling based heuristics, Rapidly-Exploring Random Trees (RRT) [32] are extensively used due to their speed and versatility. As a result, variations have been developed to improve their computational performance and optimality. Kothari et al. [33] explored the use of RRT for path planning of multiple UAVs in obstacle-rich 2D environments. Lin & Saripalli [34] present RRT with Dubins curves for static and dynamic obstacles in 3D space. Pharpatara et al. [35] used the RRT* combined with a potential field that bias sampling to plan fixed-wing UAV flight paths. Lin & Saripalli [36] implemented an RRT for collision avoidance, allowing the vehicle to edit intermediate waypoints in the event of incoming conflicts.

The reviewed routing algorithms assume that flight paths are fixed and predetermined, and therefore omit avoidance requirements that would affect energy consumption patterns and overall operational performance. Despite our extensive review of UAV logistics literature (Table 1), to the best of our knowledge, no study has so far developed a holistic approach to UAV-based humanitarian mission design. We address this gap by developing an integrated trajectory-location-routing model that determines optimal UAV trajectories for relief distribution, supported by optimally determined operational hubs. In structuring this framework, we identified two operational components driving the decision considered in this paper:

- UAV operations component, focusing on the development and improvement of trajectories, considering aerodynamic effects, varying payloads, energy requirements, terrain topography and moving obstacles. Travel times and energy requirements are used to calculate variable transportation costs at the humanitarian mission design stage.
- Humanitarian operations component, focusing on the design of the relief cargo supply chain and the selection of optimal warehouse depots. The location of depots and structure of deliveries is determined with the objective of minimising supply times and the overall duration of the humanitarian mission.

The two components are integrated as a bi-level optimisation framework, where the humanitarian component evaluates operational performance based on cost and material transported. The UAV operations component estimates payloads, endurance, ensures safety conditions and considers the variable energy demands associated with changes in flight height. Unique features of our approach include the consideration of potential conflicts, payload quantities, terrain geography and fuel consumption rates for hybrid UAV operations. Further features include the use of multiple distribution hubs (for goods distribution and battery/fuel storage) and the consideration of a range of vehicle routing objectives (energy management, split deliveries), defined as a dynamic MILP LRP solved using a bi-level Large Neighbourhood Search algorithm, containing an Informed RRT* (I-RRT*) algorithm that re-plans trajectories in the event of conflict with another aircraft. We present the integrated trajectory-location-routing optimisation formulation in Section III, solved using the heuristic presented in Section IV. A numerical case study focusing on a hypothetical UAV-based response to the 1999 Chi-Chi earthquake in Taiwan is presented in Section V. Conclusions and recommendations for future work are provided in Section VI.

Table 1 Classification of reviewed literature.

Focus	Author	Level	Approach	Features
Trajectory	Forsmo [27]	TL	ES	Wind
	Kothari et al. [33]	OL	RT	Multiple Vehicles; Avoidance
	Lin & Saripalli [34]	OL	RT	Replanning; Avoidance
	Pharpatara et al. [35]	SL	RT	Avoidance (Static)
	Lin & Saripalli [36]	TL	RT	Avoidance
Routing	Nedjati et al. [18]	OL	GA	Scheduling; Capacity
	Dorling et al. [20]	TL	SA	Energy
	Özdamar [37]	OL	BE	Capacity; Refuelling; Split Delivery
	Murray & Chu [17]	OL	OH	Heterogeneous Fleet
	Coelho et al. [19]	OL	OH	Refuelling; Capacity
	Furini et al. [31]	OL	OH	Airspace Conflict
LR	Laporte et al. [22]	SL	ES	Capacity
	Sarıçiçek & Akkus [23]	TL	BE	Allocation
	Fikar et al. [24]	TL	OH	Heterogeneous Fleet
	Mourelo et al. [25]	TL	GA	Heterogeneous Fleet
	Kim et al. [38]	TL	OH	Capacity
ITLR	This study	OL	OH	Refuelling; Split Delivery; Battery Modelling; Avoidance

Table Legend
Focus: LR - Location-Routing, ITLR - Integrated Trajectory-Location-Routing.
Operational Level: TL – Tactical Level, OL – Operational Level, SL – Strategic Level
Solution Method: ES – Exact Solution, BE – Bi-stage Exact Solution, GA – Genetic Algorithm, SA – Simulated Annealing, RT – Rapidly Exploring Random Tree, OH – Other Heuristic

III. Model Formulation

We aim to determine the optimal location of warehouses, as well as the schedule and flight routes the UAVs will follow. Our proposed model is an integrated trajectory-location-routing optimisation model that considers aspects of un-capacitated hubs, a time-dependent Green VRP with multiple hubs, split deliveries and path re-planning. The objective is to minimise the mission time and number of hubs for a pre-defined amount of relief cargo. We adopt the following assumptions:

Assumption 1: VTOL-capable battery-powered hybrid UAVs used.
This assumption is based on the recent widespread adoption of hybrid UAVs for logistics and broad development of battery-powered UAVs (which constitute 96% of the market [39]). Their precision and control permit operation in the absence of runways for take-off and landing, rendering them particularly useful in infrastructure-deficient environments. Additionally, we assume low velocities and insignificant air resistance effects during VTOL.

Assumption 2: Beyond Visual Line of Sight (BVOS) operations are allowed.
EASA proposes that small UAVs cannot operate BVOS in civilian settings [40]. Given that UAVs operate within their suggested altitude range, we assume that a reasonable relaxation of the rule is provided for humanitarian operations. There is a record of such deployments in Rwanda [41], with WFP-led efforts to develop regulations for UAV humanitarian response being ongoing at the time of writing [42].

Assumption 3: UAVs have an aggregate efficiency constant μ.
We adopt an efficiency parameter of μ that aggregates propeller, motor and battery efficiencies [43]. The latter vary continuously during flight, and are affected by vehicle velocity, electric current, temperature, among others [44–46]. As such, we consider the definition of accurate mathematical models for the efficiency parameters beyond the scope of this study.

Assumption 4: The difference between true and indicated airspeeds is negligible.
We considered true airspeed (actual movement of the aircraft relative to the air mass) to be equal to indicated airspeed

(measured speed of the vehicle). The impact of this assumption is minimal, as vehicles considered travel below sonic speed and air density variations with sea level can be ignored [47]. However, this assumption excludes the impact of weather effects and wind speeds, which lie beyond the scope of this study.

Assumption 5: A unitised commodity type is provided throughout the operation.

Relief operations commonly rely on standardised supply kits that are developed for specific incident type (earthquake, flooding, displacement), demography (diet, religion) and climate combinations. This practice is used to simplify the logistics of disaster response, as only a single commodity needs to be stocked, transported and distributed [48].

Assumption 6: Battery replacement times are negligible.

We consider battery replacement times to be negligible compared to overall mission durations. This follows from previous work on the design of autonomous systems with immediate replacements [49–51] and the availability of UAV models with easily accessible battery compartments, such as eBee [52] and DeltaQuad [53].

Assumption 7: Battery replacements are available at all hubs.

Fuel management optimisation is considered outside the scope of this study in the interest of pursuing numerical results. It is acknowledged that the provision of sufficient battery replacements would require an increased initial investment. However, considering the small fleet size presented in this study, the excess batteries will comprise a minimal impact on the total response cost.

Assumption 8: Hubs are un-capacitated.

This assumption was made given the relative difference in scales between the proposed method and common humanitarian operations, which typically ascend to several tonnes of relief cargo [54, 55]. Therefore, we assume that the hubs to be used provide sufficient cargo capacity to undertake the full UAV response.

Assumption 9: Flight data is accessible within the fleet.

Vehicles share information on trajectory and speed, facilitating collision avoidance. The assumption is made given the deployment of the UAV fleet by a single actor, so it is reasonable to assume that data sharing is bi-directional.

A. Model Formulation

We present the objective function (1) that integrates multiple aspects of humanitarian response under a unitised cost value, Z. The algorithm considers four factors described in (1.1-1.4):

$$\text{Minimise} \quad Z = HC + FC + BC + DP \tag{1}$$

$$HC = \sum_{i \in \mathcal{H}} (h_i F + \sum_{j \in \mathcal{N}} \sum_{v \in \mathcal{V}} \sum_{t \in \mathcal{T}} c_{i,j,v,t} \sigma) \tag{1.1}$$

$$FC = \sum_{t \in \mathcal{T}} \sum_{i,j \in \mathcal{N}} r_{i,j,v,t} \Delta t_{i,j,t} C \tag{1.2}$$

$$BC = \sum_{t \in \mathcal{T}} \sum_{i,j \in \mathcal{N}} r_{i,j,v,t} SOC_{i,j,t,e_f} B_c \tag{1.3}$$

$$DP = \sum_{i \in \mathcal{N}} (p_i + s_i) Pen \tag{1.4}$$

Equation (1.1) considers the costs of setting up a depot in node i. We use a per-depot cost F across all nodes and an item related cost σ, that incorporates costs associated with hub capacity. Total mission durations are captured by equation (1.2), which calculates the total flight costs given a value time C. Further flight costs are considered by accounting for battery depletion costs in equation (1.3). Finally, we introduce a numerical penalty Pen (1.4) associated with the loss of a life that could be attributed to a late or missed delivery of planned relief cargo units. The Pen parameter in this study operates similarly to the Big M method, therefore forcing the model to prioritise mission completion [56]. The formulation of the model is then as follows:

$$\text{Minimise} \quad Z = HC + FC + BC + DP \tag{2}$$

Subject to:

$$\sum_{j \in \mathcal{N}: t + \Delta t_{i,j,t} < \mathcal{T}} r_{j,i,v,t} - \sum_{j \in \mathcal{N}: t + \Delta t_{i,j,t} < \mathcal{T}} r_{i,j,v,t+\Delta t_{i,j,t}} = 0 \qquad \forall i \in \mathcal{N}, \ \forall v \in \mathcal{V}, \ \forall t \in \mathcal{T} \tag{2.1}$$

$$r_{i,i,v,t} = 0 \qquad \forall i \in \mathcal{D},\ \forall v \in \mathcal{V},\ \forall t \in \mathcal{T} \tag{2.2}$$

$$\sum_{t\in\mathcal{T}}\sum_{v\in\mathcal{V}}\sum_{j\in\mathcal{N}} r_{j,i,v,t} - \sum_{t\in\mathcal{T}}\sum_{v\in\mathcal{V}}\sum_{j\in\mathcal{N}} r_{i,j,v,t} = 0 \qquad \forall i \in \mathcal{N} \tag{2.3}$$

$$\sum_{t-\Delta t_{i,j,t}\in\mathcal{T}}\sum_{i\in\mathcal{N}}\sum_{j\in\mathcal{N}} r_{i,j,v,t} = 1 \qquad \forall v \in \mathcal{V} \tag{2.4}$$

$$\sum_{i\in\mathcal{H}}\sum_{j\in\mathcal{N}} r_{i,j,v,t_0} = 1 \qquad \forall v \in \mathcal{V} \tag{2.5}$$

$$\sum_{i\in\mathcal{N}}\sum_{j\in\mathcal{H}} r_{i,j,v,t_f} = 1 \qquad \forall v \in \mathcal{V} \tag{2.6}$$

$$\sum_{i\in\mathcal{N}} h_i \geq 1 \tag{2.7}$$

$$\sum_{j\in\mathcal{N}:t+\Delta t_{i,j,t}<\mathcal{T}} c_{j,i,v,t} - \sum_{j\in\mathcal{N}:t+\Delta t_{i,j,t}<\mathcal{T}} c_{i,j,v,t+\Delta t_{i,j,t}} \geq 0 \qquad \forall i \in \mathcal{D},\ \forall v \in \mathcal{V},\ \forall t \in \mathcal{T} \tag{2.8}$$

$$\sum_{t\in\mathcal{T}}\sum_{v\in\mathcal{V}}\sum_{j\in\mathcal{N}} c_{j,i,v,t} - \sum_{t\in\mathcal{T}}\sum_{v\in\mathcal{V}}\sum_{j\in\mathcal{N}} c_{i,j,v,t} + u_i = A_i \qquad \forall i \in \mathcal{N} \tag{2.9}$$

$$s_i - p_i = u_i \qquad \forall i \in \mathcal{N} \tag{2.10}$$

$$r_{i,j,v,t}Q \geq c_{i,j,v,t} \qquad \forall i,j \in \mathcal{N},\ \forall v \in \mathcal{V},\ \forall t \in \mathcal{T} \tag{2.11}$$

$$b_{v,0} = 0 \qquad \forall v \in \mathcal{V} \tag{2.12}$$

$$e_{v,t+1} = \left(1 - \sum_{i\in\mathcal{N}}\sum_{j\in\mathcal{H}} r_{i,j,v,t}\right)\left(e_{v,t} + \sum_{i\in\mathcal{N}}\sum_{j\in\mathcal{N}} SOC_{i,j,t,e_f} r_{i,j,v,t}\right) \qquad \forall v \in \mathcal{V},\ \forall t \in \mathcal{T} \tag{2.13}$$

$$e_{v,t} + \sum_{i,j\in\mathcal{N}} SOC_{i,j,t,e_f} r_{i,j,v,t} \leq 1 \qquad \forall v \in \mathcal{V},\ \forall t \in \mathcal{T} \tag{2.14}$$

$$x_{i,j,t,e+1} = x_{i,j,t,e} + \Delta e_{i,j,t} U_{i,j,t,e} cos(\gamma_{i,j,t,e}) cos(\psi_{i,j,t,e}) \qquad \forall i,j \in \mathcal{N},\ \forall t \in \mathcal{T},\ \forall e \in \mathcal{E} \tag{2.15}$$

$$y_{i,j,t,e+1} = y_{i,j,t,e} + \Delta e_{i,j,t} U_{i,j,t,e} cos(\gamma_{i,j,t,e}) sin(\psi_{i,j,t,e}) \qquad \forall i,j \in \mathcal{N},\ \forall t \in \mathcal{T},\ \forall e \in \mathcal{E} \tag{2.16}$$

$$z_{i,j,t,e+1} = z_{i,j,t,e} + \Delta e_{i,j,t} U_{i,j,t,e} sin(\gamma_{i,j,t,e}) \qquad \forall i,j \in \mathcal{N},\ \forall t \in \mathcal{T},\ \forall e \in \mathcal{E} \tag{2.17}$$

$$SOC_{i,j,t,e+1} = SOC_{i,j,t,e} - \frac{\Delta e_{i,j,t} T_{i,j,t,e} U_{i,j,t,e}}{\mu BV} \qquad \forall i,j \in \mathcal{N},\ \forall t \in \mathcal{T},\ \forall e \in \mathcal{E} \tag{2.18}$$

$$mU_{i,j,t,e} = T_{i,j,t,e} - D_{i,j,t,e} + W sin(\gamma_{i,j,t,e}) \qquad \forall i,j \in \mathcal{N},\ \forall t \in \mathcal{T},\ \forall e \in \mathcal{E} \tag{2.19}$$

$$D_{i,j,t,e} = \frac{1}{2}\rho U^2_{i,j,t,e} S C_{D_{i,j,t,e}} \qquad \forall i,j \in \mathcal{N},\ \forall t \in \mathcal{T},\ \forall e \in \mathcal{E} \tag{2.20}$$

$$C_{D_{i,j,t,e}} = C_{D0} + KC^2_{L_{i,j,t,e}} \qquad \forall i,j \in \mathcal{N},\ \forall t \in \mathcal{T},\ \forall e \in \mathcal{E} \tag{2.21}$$

$$C_{L_{i,j,t,e}} = \frac{n_{i,j,t,e} W}{\frac{1}{2}\rho U^2_{i,j,t,e} S} \qquad \forall i,j \in \mathcal{N},\ \forall t \in \mathcal{T},\ \forall e \in \mathcal{E} \tag{2.22}$$

$$n^2_{i,j,t,e} = n^2_{v_{i,j,t,e}} + n^2_{h_{i,j,t,e}} \qquad \forall i,j \in \mathcal{N},\ \forall t \in \mathcal{T},\ \forall e \in \mathcal{E} \tag{2.23}$$

$$\psi_{i,j,t,e+1} = \psi_{i,j,t,e} + \Delta e_{i,j,t,e} \frac{g n_{h_{i,j,t,e}}}{U_{i,j,v,t} cos(\gamma_{i,j,t,e})} \qquad \forall i,j \in \mathcal{N},\ \forall t \in \mathcal{T},\ \forall e \in \mathcal{E} \tag{2.24}$$

$$\gamma_{i,j,t,e+1} = \gamma_{i,j,t,e} + \Delta e_{i,j,t,e} \frac{g}{U_{i,j,v,t}}(n_{v_{i,j,t,e}} - cos(\gamma_{i,j,t,e})) \qquad \forall i,j \in \mathcal{N},\ \forall t \in \mathcal{T},\ \forall e \in \mathcal{E} \tag{2.25}$$

$$\Delta t_{i,j,t} = \sum_{e\in\mathcal{E}} \Delta e_{i,j,t.e} \qquad \forall i,j \in \mathcal{N},\ \forall t \in \mathcal{T} \tag{2.26}$$

$$(x_{i,j,t,e} - x_{k,l,t,s})^2 + (y_{i,j,t,e} - y_{k,l,t,s})^2 \geq R^2_{xy} \qquad \forall i,j,k,l \in \mathcal{N},\ \forall t \in \mathcal{T},\ \forall e,s \in \mathcal{E} \tag{2.27}$$

$$(z_{i,j,t,e} - z_{k,l,t,s})^2 \geq R^2_z \qquad \forall i,j,k,l \in \mathcal{N},\ \forall t \in \mathcal{T},\ \forall e,s \in \mathcal{E} \tag{2.28}$$

$$r_{i,j,t,e} \in [0,1],\ \ c_{i,j,t,e} \in [0,1,\ldots] \qquad \forall i,j \in \mathcal{N},\ \forall t \in \mathcal{T},\ \forall e \in \mathcal{E} \tag{2.29}$$

$$s_i \in [0,1,\ldots,A_i], p_i \in [0,1,\ldots,A_i] \qquad \forall i \in \mathcal{N} \tag{2.30}$$

$$h_i \in [0,1], \quad u_i \in [-A_i, \ldots, A_i] \qquad \forall i \in \mathcal{N} \tag{2.31}$$

$$|\gamma_{i,j,t,e}| \leq \frac{\pi}{2}, |\psi_{i,j,t,e}| \leq \pi, 0 \leq T_{i,j,t,e} \leq T_{max}, U_{i,j,t,e} = U_c \qquad \forall i,j \in \mathcal{N}, \ \ \forall t \in \mathcal{T}, \ \ \forall e \in \mathcal{E} \tag{2.32}$$

$$f(x_{i,j,t,e}, y_{i,j,t,e}) + z_{min} \leq z_{i,j,t,e} \leq f(x_{i,j,t,e}, y_{i,j,t,e}) + z_{max} \qquad \forall i,j \in \mathcal{N}, \ \ \forall t \in \mathcal{T}, \ \ \forall e \in \mathcal{E} \tag{2.33}$$

$$|\psi_{i,j,t,e+1} - \psi_{i,j,t,e}|\Delta e_{i,j,t} < \dot{\psi}_{max}, \ \ |\gamma_{i,j,t,e+1} - \gamma_{i,j,t,e}|\Delta e_{i,j,t} < \dot{\gamma}_{max} \qquad \forall i,j \in \mathcal{N} \forall t \in \mathcal{T}, \forall e \in \mathcal{E} \tag{2.34}$$

Constraint (2.1) ensures that vehicles persistently travel to a new destination immediately after arrival. Wait at a location is only allowed at hubs under constraint (2.2). Vehicle conservation is enforced by equation (2.3), while (2.4) ensures that no new destinations are selected until its current trip is completed. Constraints (2.5-2.6) indicate that vehicles must start and end the mission at a hub. The final solution must contain at least one hub as defined by equation (2.7).

Constraint (2.8) ensures material is only collected from hubs. Mass balance is enforced by equation (2.9), where supply is defined as a negative demand in A_i. The behaviour of u_i is linearised in (2.10) by introducing two slack variables. Finally, equation (2.11) cargo is only assigned at vehicle flows ($r_{i,j,v,t} = 1$) with each carrying a maximum capacity Q.

Constraints (2.12-2.14) describe the battery constraints. The percentage battery use b is initialised at 0 by (2.12). Equation (2.13) describes the battery expenditure when travelling through the network. The first term allows the battery to be recharged when accessing a hub. Constraint (2.14) ensures that battery level is kept below maximum capacity

Equations (2.15-2.28) define UAV flight constraints under the 3D Cartesian coordinate system defined in (2.15-2.17). Battery depletion during flight is described in (2.18), the value of which is used in (2.13). Vehicle thrust is calculated using the point mass model flight equilibrium equation defined in (2.19). Equation (2.20) describes the drag force relation to the drag coefficient, the latter defined as a function of C_L in (2.21). Equation (2.22) relates C_L and load factor n, which varies with turning as described by (2.23-2.25). Total flight time is calculated by equation (2.26). Constraints (2.27-2.28) ensure non-conflicting trajectories are developed, considering horizontal and vertical safety distances respectively.

Finally, Constraints (2.29-2.31) describe $r_{i,j,v,t}$ and h_i as Boolean variables, and limit $c_{i,j,v,t}$, u_i, p_i and s_i to integer values. We limit flight path angle to 90 degrees, and assume that thrust T is positive and lower than the maximum thrust level provided by motors in (2.32). Additionally, the target speed U_{cr} is predetermined and fixed throughout the cruise stage. We consider a variable terrain geography in constraint (2.33), described by function $f(x_{i,j}, y_{i,j})$, assuming a fixed ground clearance z_{min} and maximum altitude z_{max}. Finally, turning is limited to maximum turning rates $\dot{\psi}_{max}$ and $\dot{\gamma}_{max}$.

We solve the above problem using the Branch and Bound algorithm provided by CPLEX with an Intel Xeon E5-1650 CPU and 32GB RAM. Given the large number of variables, only small problem instances that did not consider trajectory management were solvable.

Table 2 Model performance for sample instances. Solutions were not obtained for missions with durations within 24-hour execution window.

Instance	Demand (kg)	Drones	Mission Time (min)	Demand Serviced (%)	Runtime (s)
3 nodes	70	5	50	No Solution	No Solution
			100	28	8
			150	100	68
	80	10	50, 100	No Solution	No Solution
			150	100	68
	100	15	50	No Solution	No Solution
			100	42	2
			150	100	112
4 nodes	70	5	50, 100	No Solution	No Solution
			150	100	205
		10	50, 100, 150	No Solution	No Solution
		15	50, 100, 150	No Solution	No Solution
5 nodes	80	5	50	7	3
			100, 150	No Solution	No Solution
		10	50	19	6
			100, 150	No Solution	No Solution
		15	50	26	26
			100, 150	No Solution	No Solution

IV. Metaheuristic solution algorithm

In this section, we present the approximate heuristic developed to overcome the computational limitations of the exact algorithm above. The heuristic is developed using the C# programming language and consists of a custom bi-layered Large Neighbourhood Search (LNS) that creates location-routing solutions. Initial trajectories are developed using a non-linear optimisation algorithm to ensure close-to-optimality, without considering potential conflicts with other UAVs. A path improvement algorithm consisting of an I-RRT* resides in the inner LNS. The structure of the heuristic is presented in Fig. 1.

The algorithm commences by initiating the outer LNS layer. A randomly generated solution-neighbourhood N_i is created where each neighbour explores a different branch of the solution space independently. At every iteration, a single solution is selected for manipulation using a fitness proportional selection method. Selected solutions are manipulated using custom destroy and repair algorithms chosen with probability rates defined in Table 3. The overall progress of the search is monitored using a temperature metric T. This represents the search space that can be explored from the best-known solution and decreases with every iteration of the LNS.

The search process and its behaviour are controlled by two parameters. The “cooling rate” c controls the speed of the LNS by determining the change rate of T. The “absolute temperature” a defines the termination point of the search process. Solutions s are evaluated using the objective function (1), generating the scalar fitness value f_s. At every iteration, parent solution s_1 is evaluated against a newly generated candidate solution s_2. The candidate s_2 replaces the parent s_1 if f_{s_2} is better than f_{s_1}, or if a random number z is smaller than probability P, where P is a function of T and fitness difference between both solutions δZ by equation (3). Otherwise, s_2 is discarded, and a new solution is generated. Replacement with an inferior solution may appear counter-intuitive but ensures that the algorithm is not limited by a local optimum. The structure of the LNS is presented in pseudocode format in Algorithm 1.

$$P = exp(-\frac{\delta Z}{T}) \tag{3}$$

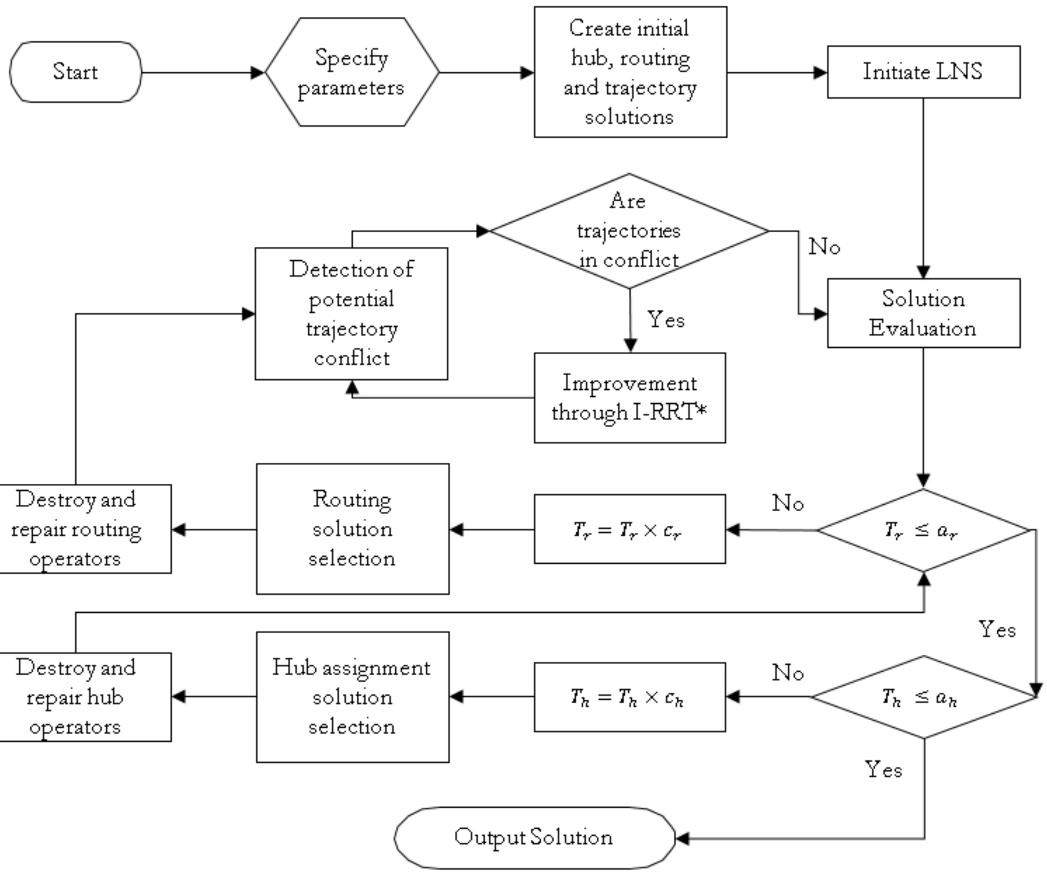

Fig. 1 Model workflow.

Algorithm 1 Large Neighbourhood Search

function MAIN LNS
    Input: temperature T, absolute temperature a, cooling rate c, neighbourhood size n
    Output: optimal solution s^*

    neighbourhood $N \leftarrow$ GenerateInitialSolution(n)
    while $T > a$ **do**
        $s_1 \leftarrow$ Selection(N, f_N)
        $s_2 \leftarrow$ Destroy(s_1)
        $s_2 \leftarrow$ Repair(s_2)
        $f_{s_2} \leftarrow$ EvaluateSolution(s_2)
        $z \leftarrow$ RandomNumber(0, 1)
        if $f_{s_2} < f_{s_1}$ **or** $z < \exp \frac{|f_{s_1} - f_{s_2}|}{T}$ **then**
            $N_{s_1} \leftarrow s_2$
        end if
        $T = cT$
    end while
    return $s^* \leftarrow$ FindMinimum(s_f)
end function

Table 3 Large Neighbourhood Search - Destroy and Repair Operators

Operator	Assignment			Routing		
	Name	Condition	Description	Name	Condition	Description
Destroy	Random	$z < \alpha_d$	Uniform randomised hub elimination.	Random	$z < \eta_d$	Deletion of uniformly randomised element in schedule.
	Utilisation	$\alpha_d \leq z$ $z < \beta_d$	Deletes hub with least packages delivered.	Demand	$\eta_d \leq z$ $z < \omega_d$	Delete most visited destination in route.
	Cost	$\beta_d \leq z$	Remove highest cost hub	Distance	$\omega_d \leq z$	Remove route segments that require greatest travel distance.
Repair	Random	$z < \alpha_r$	Uniform randomised hub selection.	Random	$z < \eta_r$	Addition of uniformly randomised destination into a random section of the schedule.
	Utilisation	$\alpha_r \leq z$ $z < \beta_r$	Selects hub closest to current demand points.	Demand	$\eta_r \leq z$ $z < \omega_r$	Add destination with least deliveries to a random section of the schedule.
	Cost	$\beta_r \leq z$	Add lowest cost hub	Combined	$\omega_r \leq z$	Adds destination with least deliveries to a the schedule section that causes least deviation in the route.

A. Trajectory Improvement Algorithm

At every generation of the LNS, hub location and routing decisions are evaluated based on potential aerial conflicts between UAVs, defined by constraints (2.27-2.28). UAVs share information on their position, speed, and expected trajectory with other vehicles within their detection radius, identifying potential threats using geometric conflict detection process.

The generation of potential conflict-free paths is performed using a custom I-RRT* algorithm (refer to Algorithm 2). The algorithm follows a similar framework to the original RRT, developed by LaValle [32]: it commences by generating a random state x_r and the closest node x_n to x_r is found. A new node x_s is generated at distance r_{step} from x_n in the direction towards x_r. Provided the link between x_n and x_s contains no collisions, x_s is added to the node tree. Our approach deviates in some key ways from the basic algorithm. Firstly, the algorithm considers kinematic constraints limiting UAV flight given constraints (2.32-2.33). In particular, vehicles are limited on their turning angle rate by $\dot{\psi}_{max}$, and pitch rate $\dot{\gamma}_{max}$. Next, the explorable area reduces linearly with every iteration to accelerate convergence. Thirdly, while the closest node x_n is found using Euclidean distance, we connect the candidate node x_s to the existing tree using battery consumption evaluating factor based on equations (2.18-2.25) as shown in Select Best procedure. Given that any changes in pitch and heading result in increased battery consumption, the algorithm naturally advantages smooth paths. Finally, the algorithm considers multiple options for path extension at each step, providing each with a score based on their proximity to obstacles and destination expressed by (4). A selection probability proportional to their score is created in (5). Finally, an iterative smoother algorithm is used to smoothen the path.

$$F_n = -(x_{d,t} - x_{n,t})^2 + (y_{d,t} - y_{n,t})^2 + \sum_{o \in O} (x_{o,t} - x_{n,t})^2 + (y_{o,t} - y_{n,t})^2 \qquad \forall n \in \mathcal{N} \tag{4}$$

$$P_n = \frac{F_n}{\sum_{n \in \mathcal{N}} F_n} \qquad \forall n \in \mathcal{N} \tag{5}$$

We test our path improvement algorithm in a $24x24km^2$ area under three conditions: in the presence of a static obstacle, a dynamic obstacle, and multiple vehicles. In the case of the first two, the detection radius of the UAV is

Algorithm 2 Informed Rapidly Exploring Random Tree *

function MainIRRT
    Input: origin node x_o, destination node x_d, vehicle v, maximum iterations θ, step radius r_{step}, neighbour radius r_n, obstacles O
    Output: path p

    U = List(x_o)
    for iteration i **in** θ **do**
        $x_r \leftarrow$ CreateNewNodes(x_o, x_d, i, θ)
        $x_n \leftarrow$ FindClosestNodes(x_r, U)
        $x_s \leftarrow$ CreateStepNodes(x_r , x_n)
        if IsEmtpy(x_s) **then continue**
        end if
        $x_b \leftarrow$ SelectBest(x_s, x_d, O)
        $x_b \leftarrow$ SetCheapestNeighbour(x_b, U, v, r_n, O)
        U.Add(x_b)
        if IsGoalReached(x_b, x_d) **then break**
        end if
    end for
    return $p \leftarrow$ ExtractPath(U)
end function

---

function Create New Nodes
    Input: origin node x_o, destination node x_d, iteration i, maximum iterations θ
    Output: candidate node x_c

    $c_1 = x_d - x_{min}$
    $c_2 = x_{max} - x_d$
    $s = \frac{i}{\theta}$
    return $x_c = rand \times (c_1 + c_2)s + x_d - c_1 s$
end function

---

function Create Step Node
    Input: candidate node x_r, near node x_n, vehicle v, step radius r_{step}
    Output: step node x_s

    $d \leftarrow$ Distance(x_r, x_n)
    if $d \geq r_{step}$ **then**
        $x_s = x_r + (x_r - x_n)\frac{r_{step}}{d}$
    end if
    pitch $\gamma \leftarrow$ GetPitch(x_s, x_n)
    bearing $\psi \leftarrow$ GetBearing(x_s, x_n)
    if $\gamma >$ maximum vehicle pitch $\dot{\gamma}_v$ **then** $\gamma = \dot{\gamma}_v$
    end if
    if $\psi >$ maximum vehicle bearing $\dot{\psi}_v$ **then** $\psi = \dot{\psi}_v$
    end if
    return $x_s \leftarrow$ GetNode(x_n, r_{step}, ψ, γ)
end function

---

function Find Closest Nodes
    Input: candidate node x_r, node list U
    Output: closest node x_n

    d_{max} = inf
    for x_c in U **do**
        if conflict $c_{x_c} \geq 1$ **then continue**
        end if
        d_n = Distance(x_c, x_r)
        if IsKinematicallyInfeasible(x_c, x_r, v) **then continue**
        end if
        if $d_n < d_{max}$ **then**
            $d_{max} = d_n$
            $x_n = x_c$
        end if
    end for
    return x_n
end function

---

function Set Cheapest Neighbour
    Input: candidate node x_r, node list U, vehicle v, neighbour radius r_n, obstacles O
    Output: step node x_s

    for x_n in U **do**
        cost c = CalculateBatteryUse(x_n, x_r, v)
        distance d = CalculateDistance(x_n, x_r)
        if $d > r_n$ **then continue**
        end if
        if IsKinematicallyInfeasible(x_s, x_r, v) **then continue**
        end if
        if CheckObstacles(x_r, O) **then continue**
        end if
        if $c_{x_r} \leq c$ **then continue**
        end if
        parent node $p_{x_r} = x_n$
        step node $x_s = x_r$
    end for
    return x_s
end function

extended such that the UAV is aware of the obstacle position even at initial planning. Additionally, the UAV must traverse from an initial position at (20,8) to destination (20,32), with the obstacle is positioned at (20,20). In the dynamic case, it is assumed that the obstacle moves towards (20,8), at a constant speed of $20m/s$, similar to the UAV cruise speed. The multi-vehicle scenario considers a safety distance of $1km$ between all UAVs to facilitate visualisation. Additionally, given the presence of multiple self-avoiding vehicles, a conflict resolution hierarchy is implemented consisting of three levels. The first level considers the expected remaining battery after landing, such that the vehicle with more battery for the next flight is responsible for manoeuvering. The second condition considers the distance towards the current destination, with vehicles closer to landing having priority. Finally, the last level compares the identification number associated with each vehicle. In all scenarios, UAVs successfully avoid incoming targets while minimising deviation from the optimal path (in all cases a simple straight path). The final trajectories are presented in Fig. 2, with time-discretised paths provided in the Appendix. A comparison between the proposed modified RRT* and the original RRT is also presented in Table 4. The I-RRT* algorithm consistently provides higher degrees of optimality than any configuration of the RRT. The improvement of RRT optimality results in prohibitive computational performance - a reduction in the optimality gap to 1% requires a 2-second runtime increment for the static obstacle instance.

Table 4 Path Replanning Algorithm Performance.

Instance		I-RRT*	RRT	RRT (2x)	RRT (3x)
Static Obstacle	Optimality Gap (%)	0	7.98	2.08	1.41
	Runtime (s)	0.395	0.361	1.316	2.852
Dynamic Obstacle	Optimality Gap (%)	0	12.95	6.56	2.23
	Runtime (s)	0.437	0.383	1.322	2.925
Multiple Vehicles	Optimality Gap (%)	0	4.97	2.47	1.64
	Runtime (s)	8.063	7.223	25.303	56.778

The bracketed number refers to the number of iterations in comparison with the proposed algorithm (I-RRT*), where x denotes the original number of iterations.

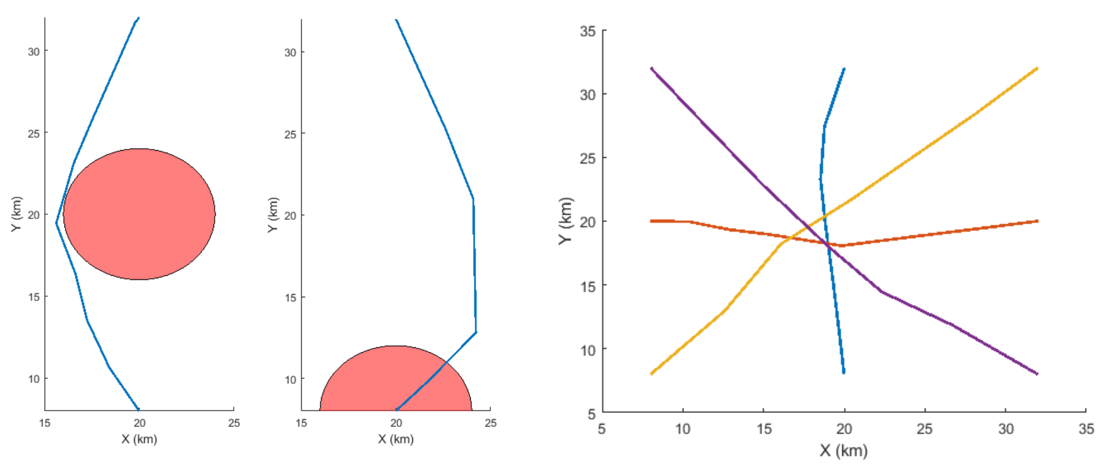

(a) Static Obstacle (b) Dynamic Obstacle (c) Multiple Vehicles

Fig. 2 Rapid Random Tree Simulation Results

V. Results and Discussion

We apply the above heuristic to a network extracted from the 1999 Chi-Chi earthquake in Taiwan. With over 2,000 casualties, 10,000 injuries and 14,000 damaged buildings, it is one of the largest disasters recorded in East Asia [57].

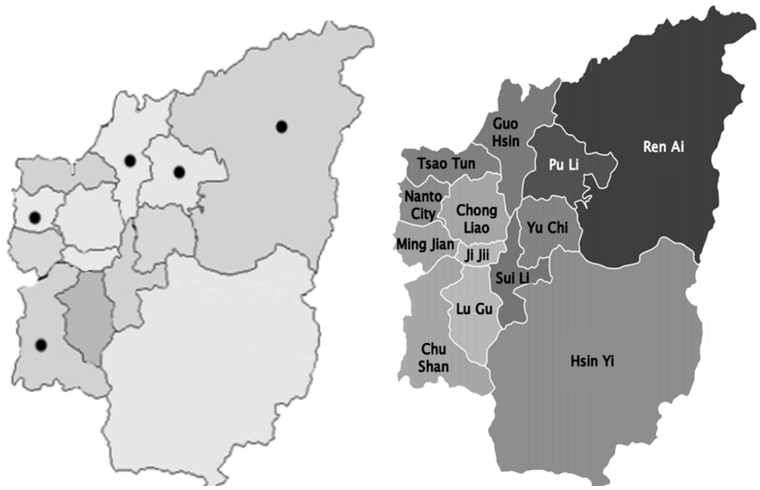

(a) Depot Locations (b) Townships

Fig. 3 Nanto County - Taiwan

Table 5 Nanto County post-earthquake data including coordinates of each warehouse.

Node	Name	Location		Population	Frail Population	Demand (kg)
		Latitude	Longitude			
1	Nanto	120.6808	23.92176	104,777	215	108
2	Ren Ai	121.1435	24.02771	15,358	298	149
3	Guo Hsin	120.8684	24.01024	24,643	567	284
4	Pu Li	120.9647	23.99367	88,271	161	80
5	Chu Shan	120.6932	23.70884	62,269	342	171

The damages and relief necessities of the central region of Nanto were captured by Sheu [58]. The dataset has since been used as a benchmark case for studies on disaster response optimisation. The presence of variable terrain and extensive infrastructure damage renders this a suitable scenario for humanitarian UAV operations. In this study, we seek to optimise the distribution of 1kg care-packages for the frail population in the northern region of Nanto, reducing the problem size in the pursuit of numerical results (refer to Fig. 3).

Optimal itineraries developed in the algorithm are represented using five data vectors. A route r specifies the order of deliveries carried out by the UAV, where each element r_i refers to an identity number similar to Table 5. A cargo assignment c_a vector defines total cargo carried to each destination r_i. A cargo delivered c_d vector denotes the total cargo delivered to each destination r_i, such that $c_{d_i} \le c_{a_i}$ and $c_{a_{i-1}} - c_{d_{i-1}} \le c_{a_i}$. Finally, a hub visit time-step vector h_t indicates at which route step i a hub is visited, noting that the visit takes part before travelling to r_i. Finally, a hub visit vector h_v indicates what hub is visited using identity integers. An indicative example of the proposed data structure is presented in table 6.

Table 6 Itinerary dataset example.

Data type	Example
Route Itinerary	1,3,4,5,1,2,4,3,5,...
Cargo Assignment	3,3,3,3,2,3,1,3,2,...
Cargo Delivered	3,3,3,1,2,2,1,3,2,...
Hub Visited (time)	1,2,3,4,6,8,9,...
Hub Visited (destination)	6,7,6,6,6,7,6,...

A. Parameter Tuning

The derivation of suitable LNS control parameters is achieved through manual tuning, using algorithm runtime and optimal fitness value to evaluate parameter suitability. The temperature T value determines the replacement probability P, which should be close to unity during the initial iterations. The absolute temperature a determines the degree of elitism in the latter stages of the algorithm selection. The speed of the algorithm is controlled by the cooling rate c and must be selected to reduce runtime without compromising optimality.

We tune location and routing parameters separately. In doing so, we reduce the problem to solely a location and routing problem by providing a partial solution for each layer. Parameters α and η increase the stochasticity of the algorithm, thus reducing the effectiveness of the destroy and repair operators, but provide new search regions to explore. Higher values β increase the probability of using utilisation-based instead of cost-based processes. Finally, lower values of ω increases the use of distance and demand-based operators, which yield higher-optimal solutions. The final parameter values are: $\alpha_r, \alpha_d, \eta_r = 0.1$, $\eta_d = 0.2$, $\beta_d, \omega_r, \omega_d = 0.6$, $\beta_r = 0.7$, $T = 100,000$, $a = 0.001$, $c = 0.9$ and $N = 50$.

B. Results

We present the results obtained in this case study in table 7. All solutions locate at least one hub between Guo Hsin, Nanto and Pu Li, which together account for 60% of the total mission demand. At least one other hub is located in the southern area of the region, connecting Chu Shan and Ren Ai. Hub location coordinates are provided in the Appendix (Table B). All missions are carried out without any unresolved conflict.

Table 7 Model Outputs.

UAVs	Hubs	Completion (hr)	Inter-arrival (avg-min)	Flight Time (avg-min)	Deliveries (kg)	
					12 hours	24 hours
5	3	40.5	50.9	15.6	315	576
10	2	21.4	25.9	15.2	648	792
15	3	16.5	18.7	14.3	708	792

A further run of the model is carried out to evaluate the impact of the trajectory re-planning algorithm on the performance parameters. The instance assumes that UAVs use pre-determined shortest paths that do not account for the position of other vehicles. As results in Table 8 indicate, this yields shorter flight times and mission completion times. However, we find that all conditions yield potential collisions between the UAVs in the fleet. A reduction in conflicts is achieved in the instance with 10 drones by establishing additional hubs.

Table 8 Model Outputs - No path replanning.

UAVs	Hubs	Unresolved Conflicts	Completion (hr)	Inter-arrival (avg-min)	Flight Time (avg-min)	Deliveries (kg)	
						12 hours	24 hours
5	3	19	39.5	45.5	13.1	396	675
10	6	6	19.4	24.3	12.5	633	792
15	3	34	16.1	18.1	15.2	734	792

The main advantage UAVs pose compared to conventional vehicles is their independence of ground infrastructure and fast delivery inter-arrival times. According to our model, a small UAV fleet is capable of providing the first delivery under 20 minutes after depot establishment. This technology thus is capable of providing essential life-saving cargo when survival rates are highest [5]. However, the small payloads limit the exclusive use of UAVs for relief distribution operations and have been used in this case study to aid the frail population. As vehicle performance improves and costs reduce, UAVs will be used in larger problems instances and other phases of humanitarian response (mapping, search and rescue).

A potential limitation of UAVs relates to weather effects on UAV performance. While temperature variations reduce the battery efficiency, wind and precipitations are the main causes for control and communication loss [59, 60].

Additionally, an energy source is required to recharge batteries at the hubs, which can be achieved through the use of generators or using alternative energy sources such as liquid fuels.

VI. Conclusion

The increasing reliance of humanitarian organisations on UAVs necessitates the development of novel methodologies that incorporate the UAV-specific operational constraints. To this effect, we present an integrated trajectory-location-routing formulation that is solved using a custom bi-layered LNS with an inner I-RRT* algorithm for path re-planning and improvement. To the best of our knowledge, this process is the first to integrate aspects of avoidance and location-routing for simultaneously for multiple vehicles. The model demonstrates that not considering aspects of re-routing results in significant deviations when evaluating the operational performance of UAVs.

Despite the operational limitations relating to weather, which significantly reduce UAV performance and control, widespread adoption of UAV-based logistics operations is expected over the next decade [61]. Their adoption rate is dependent on the regulatory developments currently lead by the Federal Aviation Authority and the European Aviation Safety Agency (EASA). In the humanitarian context, WFP is developing coordination mechanisms for the integration of UAVs in disaster response [62]. Apart from building operational capacity in disaster-prone countries, WFP is working with governments towards the development of regulatory frameworks.

The presented algorithm provides re-planning capabilities to resolve interactions with vehicles within the fleet. However, interaction with other aircraft is not considered, as well as demand uncertainty aspects and the inclusion of further supply chain levels. These shall be the focus of our future work.

Appendix

Table A Heuristic performance for sample instances.

Instance	Demand (kg)	Drones	Mission Completion Time (min)	Runtime (h)
3 nodes	70	5	42	1.09
		10	24	1.12
		15	18	1.28
4 nodes	70	5	44	1.54
		10	27	1.57
		15	19	1.63
5 nodes	80	5	41	1.81
		10	24	1.90
		15	14	1.96

Table B Operational Warehouse Locations.

	5 Drones		10 Drones		15 Drones	
	Easting	Northing	Easting	Northing	Easting	Northing
Depot 1	120.7386	23.98783	120.8543	23.90813	120.8543	23.908133
Depot 2	120.8543	23.74870	121.0857	23.82842	120.8543	23.98785
Depot 3	120.8543	23.82842	-	-	120.97	23.7487

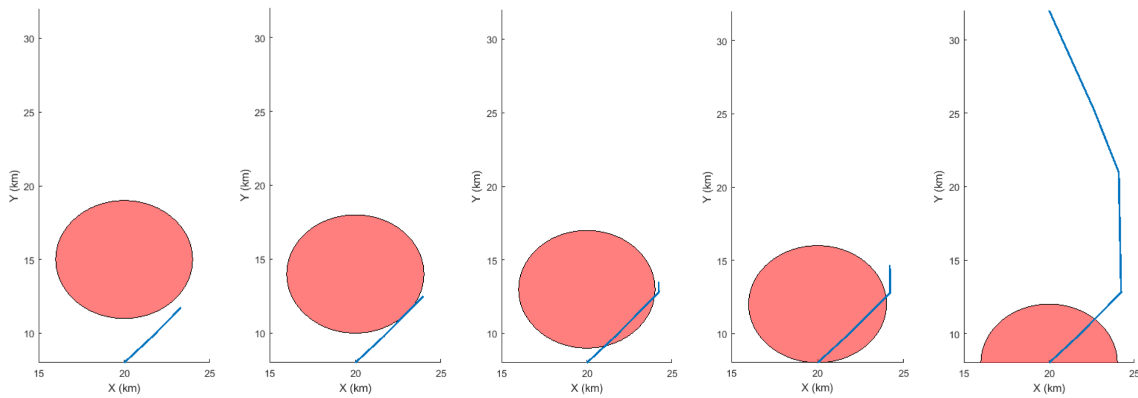

(a) t = 585 (b) t = 675s (c) t = 720s (d) t = 810s (e) t = end

Fig. A Dynamic obstacle problem chronology.

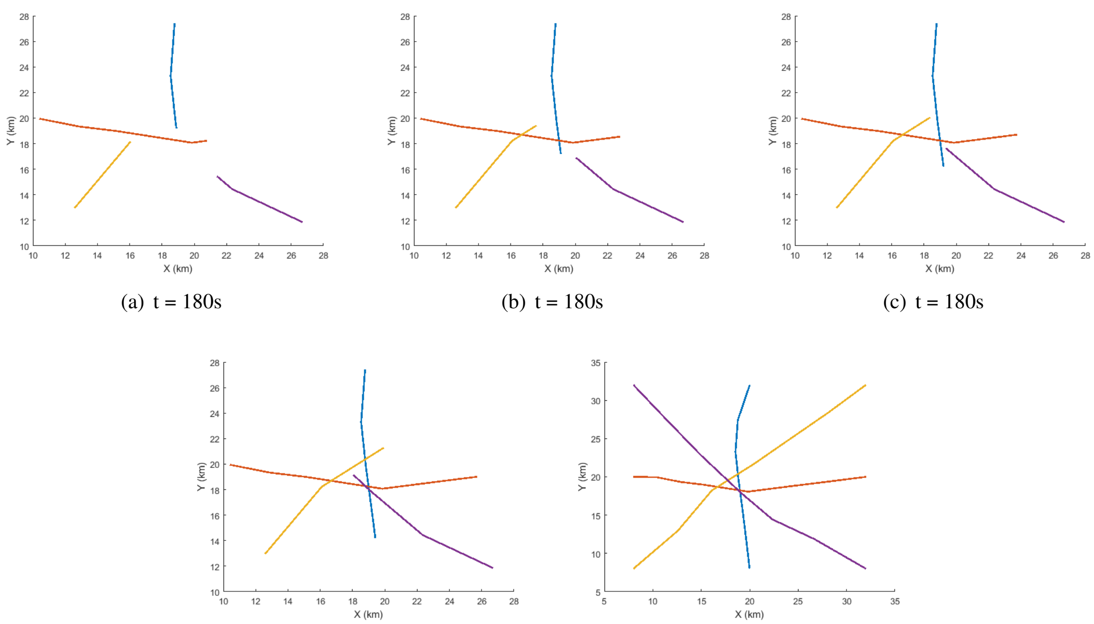

(a) t = 180s (b) t = 180s (c) t = 180s

(d) t = 180s (e) t = 180s

Fig. B Multiple vehicle problem chronology.

Acknowledgments

The research was supported by the UK Engineering and Physical Sciences Research Council (EPSRC) as part of the Sustainable Civil Engineering Centre for Doctoral Training (Grant number P/L016826/1).

References

[1] UNISDR, "Briefing Note 01 - Climate Change and Disaster Risk Reduction," Tech. Rep. September, United Nations, Geneva, Switzerland, 2008.

[2] WFP Aviation, "Annual Review 2011," Tech. rep., WFP Aviation, Rome, Italy, 2012. URL http://documents.wfp.org/stellent/groups/public/documents/communications/wfp247741.pdf?_ga=2.8805693.940050920.1519661951-2078292071.1519661951.

[3] WFP Aviation, "WFP Aviation in 2015," Tech. rep., World Food Programme, Rome, Italy, 2016. URL http://documents.wfp.org/stellent/groups/public/documents/communications/wfp284702.pdf?_ga=2.101328514.2089474537.1519309844-1504303459.1517938603.

[4] WFP, "The Year in Review 2016," Tech. rep., WFP, Rome, Italy, 2017. URL https://docs.wfp.org/api/documents/WFP-0000019183/download/?_ga=2.245347461.1698952705.1512920441-1272578713.1499352257.

[5] Huang, J. S., and Lien, Y. N., "Challenges of emergency communication network for disaster response," *2012 IEEE International Conference on Communication Systems, ICCS 2012*, 2012, pp. 528–532. doi:10.1109/ICCS.2012.6406204.

[6] Meier, P., Soesilo, D., and Guerin, D., "Cargo Drones in Humanitarian Contexts Meeting Summary," Tech. rep., FSD - Swiss Foundation for Mine Action, Sheffield, UK, 2016. URL http://drones.fsd.ch/wp-content/uploads/2016/08/CargoDrones-MeetingSummaryfinal.pdf.

[7] Van Wassenhove, L. N., and Pedraza Martinez, A. J., "Using OR to adapt supply chain management best practices to humanitarian logistics," *International Transactions in Operational Research*, Vol. 19, No. 1-2, 2012, pp. 307–322. doi:10.1111/j.1475-3995.2011.00792.x.

[8] Soesilo, D., Meler, P., Lessard-Fontaine, A., Du Plessis, J., Stuhlberger, C., and Fabbroni, V., "Drones in Humanitarian Action. A guide to the use of airbirne systems in humanitarian crises," Tech. rep., FSD, Geneva, Switzerland, 2016. URL http://drones.fsd.ch/wp-content/uploads/2016/11/Drones-in-Humanitarian-Action.pdf.

[9] Griffin, A., "Amazon Prime Air will now deliver things to people on a drone, almost straight away," , 12 2016. URL http://www.independent.co.uk/life-style/gadgets-and-tech/news/amazon-prime-air-drone-30-minute-deliveries-delivery-now-flying-a7474541.html.

[10] Afrotech EPFL, "Red Line," , 2016. URL http://afrotech.epfl.ch/page-115280-en.html.

[11] DHL, "Successful Trial Integration of DHL Parcelcopter into Logistics Chain," , 2015. doi:10.5235/204976114814222476, URL http://www.dhl.com/en/press/releases/releases_2016/all/parcel_ecommerce/successful_trial_integration_dhl_parcelcopter_logistics_chain.html.

[12] Welch, C., "Zookal will deliver textbooks using drones in Australia next year," , 2015. URL https://www.theverge.com/2013/10/15/4840706/zookal-will-deliver-textbooks-with-drones-in-australia.

[13] Meier, P., and Soesilo, D., "Using Drones for Medical Payload Delivery in Papua New Guinea," Tech. rep., FSD - Swiss Foundation for Mine Action, Geneva, Switzerland, 2014. URL http://drones.fsd.ch/wp-content/uploads/2016/04/Case-Study-No2-PapuaNewGuinea.pdf.

[14] Meier, P., "Field Testing Medical Cargo Drones in the DR," , 2018. URL https://werobotics.org/blog/2018/02/27/testing-cargo-drones-dr/.

[15] European Commission, "Press release - Aviation: Commission is taking the European drone sector to new heights," , 2017. URL http://europa.eu/rapid/press-release_IP-17-1605_en.htm.

[16] Prevot, T., Rios, J., Kopardekar, P., Robinson III, J. E., Johnson, M., and Jung, J., "UAS Traffic Management (UTM) Concept of Operations to Safely Enable Low Altitude Flight Operations," *16th AIAA Aviation Technology, Integration, and Operations Conference*, 2016, pp. 1–16. doi:10.2514/6.2016-3292, URL http://arc.aiaa.org/doi/10.2514/6.2016-3292.

[17] Murray, C. C., and Chu, A. G., "The flying sidekick traveling salesman problem: Optimization of drone-assisted parcel delivery," *Transportation Research Part C: Emerging Technologies*, Vol. 54, 2015, pp. 86–109. doi:10.1016/j.trc.2015.03.005.

[18] Nedjati, A., Vizvari, B., and Izbirak, G., "Post-earthquake response by small UAV helicopters," *Natural Hazards*, Vol. 80, 2015, pp. 1669–1688. doi:10.1007/s11069-015-2046-6.

[19] Coelho, B. N., Coelho, V. N., Coelho, I. M., Ochi, L. S., K, R. H., Zuidema, D., Lima, M. S. F., and Adilson, R., "A multi-objective green UAV routing problem," *Computers & Operations Research*, Vol. 0, 2017, pp. 1–10.

[20] Dorling, K., Heinrichs, J., Messier, G. G., and Magierowski, S., "Vehicle Routing Problems for Drone Delivery," *IEEE Transactions on Systems, Man, and Cybernetics: Systems*, Vol. 47, No. 1, 2017, pp. 70–85. doi:10.1109/TSMC.2016.2582745.

[21] Perl, J., and Daskin, M. S., "A warehouse location-routing problem," *Transportation Research Part B*, Vol. 19, No. 5, 1985, pp. 381–396. doi:10.1016/0191-2615(85)90052-9.

[22] Laporte, G., Nobert, Y., and Arpin, D., "An exact algorithm for solving a capacitated location-routing problem," *Annals of Operations Research*, Vol. 6, No. 9, 1986, pp. 293–310. doi:10.1007/BF02023807.

[23] Sarıçiçek, I., and Akkus, Y., "Unmanned Aerial Vehicle hub-location and routing for monitoring geographic borders," *Applied Mathematical Modelling*, Vol. 39, 2013, pp. 3939–3953. doi:10.1016/j.apm.2014.12.010.

[24] Fikar, C., Gronalt, M., and Hirsch, P., "A decision support system for coordinated disaster relief distribution," *Expert Systems with Applications*, Vol. 57, 2016, pp. 104–116. doi:10.1016/j.eswa.2016.03.039.

[25] Ferrandez, S. M., Harbison, T., Weber, T., Sturges, R., and Rich, R., "Optimization of a truck-drone in tandem delivery network using k-means and genetic algorithm," *Journal of Industrial Engineering and Management*, Vol. 9, No. 2, 2016, pp. 374–388. doi:10.3926/jiem.1929.

[26] Kim, J., and Morrison, J. R., "On the concerted design and scheduling of multiple resources for persistent UAV operations," *Journal of Intelligent and Robotic Systems: Theory and Applications*, Vol. 74, No. 1-2, 2014, pp. 479–498. doi:10.1007/s10846-013-9958-8.

[27] Forsmo, E. J., "Optimal Path Planning for Unmanned Aerial Systems," Ph.D. thesis, Norwegian University of Science and Technology Norway, 2012.

[28] Kim, J., Song, B. D., and Morrison, J. R., "On the scheduling of systems of UAVs and fuel service stations for long-term mission fulfillment," *Journal of Intelligent and Robotic Systems: Theory and Applications*, Vol. 70, No. 1-4, 2013, pp. 347–359. doi:10.1007/s10846-012-9727-0.

[29] Manyam, S. G., Rathinam, S., Darbha, S., and Obermeyer, K. J., "Computation of a Lower Bound for a Vehicle Routing Problem With Motion Constraints," *IEEE Conference on Decision and Control December*, Florence, Italy, 2013, pp. 2378–2383. doi:10.1115/DSCC2012-MOVIC2012-8713, URL http://proceedings.asmedigitalcollection.asme.org/proceeding.aspx?doi=10.1115/DSCC2012-MOVIC2012-8713.

[30] Mathew, N., Smith, S. L., and Waslander, S. L., "Planning Paths for Package Delivery in Heterogeneous Multirobot Teams," *IEEE Transactions on Automation Science and Engineering*, Vol. 12, No. 4, 2015, pp. 1298–1308. doi:10.1109/TASE.2015.2461213.

[31] Furini, F., Persiani, C. A., and Toth, P., "The Time Dependent Traveling Salesman Planning Problem in Controlled Airspace," *Transportation Research Part B: Methodological*, Vol. 90, 2016, pp. 38–55. doi:10.1016/j.trb.2016.04.009.

[32] LaValle, S. M., "Rapidly-Exploring Random Trees: A New Tool for Path Planning," Ph.D. thesis, Iowa State Universtity, 1998. doi:10.1.1.35.1853, URL http://scholar.google.com/scholar?hl=en&btnG=Search&q=intitle:Rapidly-exploring+random+trees:+A+new+tool+for+path+planning#0.

[33] Kothari, M., Postlethwaite, I., and Gu, D. W., "Multi-UAV path planning in obstacle rich environments using rapidly-exploring random trees," *Proceedings of the IEEE Conference on Decision and Control*, , No. December, 2009, pp. 3069–3074. doi:10.1109/CDC.2009.5400108.

[34] Lin, Y., and Saripalli, S., "Path planning using 3D Dubins Curve for Unmanned Aerial Vehicles," *2014 International Conference on Unmanned Aircraft Systems (ICUAS)*, , No. October 2016, 2014, pp. 296–304. doi:10.1109/ICUAS.2014.6842268, URL http://ieeexplore.ieee.org/document/6842268/.

[35] Pharpatara, P., Herisse, B., and Bestaoui, Y., "3-D Trajectory Planning of Aerial Vehicles Using RRT," *IEEE Transactions on Control Systems Technology*, Vol. 25, No. 3, 2017, pp. 1116–1123. doi:10.1109/TCST.2016.2582144.

[36] Lin, Y., and Saripalli, S., "Sampling-Based Path Planning for UAV Collision Avoidance," *IEEE Transactions on Intelligent Transportation Systems*, Vol. 18, No. 11, 2017, pp. 3179–3192. doi:10.1109/TITS.2017.2673778.

[37] Özdamar, L., "Planning helicopter logistics in disaster relief," *OR Spectrum*, Vol. 33, No. 3, 2011, pp. 655–672. doi:10.1007/s00291-011-0259-y.

[38] Kim, S. J., Lim, G. J., Cho, J., and Côté, M. J., "Drone-Aided Healthcare Services for Patients with Chronic Diseases in Rural Areas," *Journal of Intelligent & Robotic Systems*, 2017, pp. 163–180. doi:10.1007/s10846-017-0548-z, URL http://link.springer.com/10.1007/s10846-017-0548-z.

[39] Drone Industry Insights, "Drone Energy Sources – Pushing the Boundaries of Electric Flight," , 2017. URL https://www.droneii.com/drone-energy-sources.

[40] EASA, "A proposal to create common rules for operating drones in Europe," Tech. Rep. September, EASA, Cologne, Germany, 2015. URL https://www.easa.europa.eu/system/files/dfu/205933-01-EASA_SummaryoftheANPA.pdf.

[41] Simmons, D., "Rwanda begins Zipline commercial drone deliveries," , 2016. URL http://www.bbc.co.uk/news/technology-37646474.

[42] Vornic, A., "Drones take flight to help end hunger," , 2017. URL https://insight.wfp.org/drones-take-flight-to-help-end-hunger-20222948e01.

[43] D'Andrea, R., "Guest Editorial. Can Drones Deliver?" *IEEE Transactions on Automation Science and Engineering*, Vol. 11, No. 3, 2014, pp. 647–648. doi:10.1109/TASE.2014.2326952.

[44] Brandt, J. B., and Selig, M. S., "Propeller Performance Data at Low Reynolds Numbers," *49th AIAA Aerospace Sciences Meeting*, , No. January, 2011, pp. 1–18. doi:10.2514/6.2011-1255.

[45] Gottlieb, I., *Practical Electric Motor Handbook*, 1st ed., Reed Educational and Professional Publishing Ltd, Oxford, United Kingdom, 1997.

[46] Linden, D., *Handbook of Batteries and Fuel Cells*, McGraw-Hill Book Co., New York, NY, United States, 1984. doi: 10.1002/9780470974001.

[47] Gracey, W., "Measurement of Aircraft Speed and Altitude," Tech. rep., NASA, Hampton, VA, 1980. URL http://www.dtic.mil/dtic/tr/fulltext/u2/a280006.pdf.

[48] WFP, "72 Hours Emergency Assessment," , 2018. URL https://www.wfp.org/72-hours-emergency-assessment.

[49] Michini, B., Toksoz, T., Redding, J., Michini, M., How, J., Vavrina, M., and Vian, J., "Automated Battery Swap and Recharge to Enable Persistent UAV Missions," *Infotech@Aerospace 2011*, American Institute of Aeronautics and Astronautics, 2011. doi:10.2514/6.2011-1405.

[50] Suzuki, K. A., Kemper Filho, P., and Morrison, J. R., "Automatic battery replacement system for UAVs: Analysis and design," *Journal of Intelligent and Robotic Systems: Theory and Applications*, Vol. 65, No. 1-4, 2012, pp. 563–586. doi:10.1007/s10846-011-9616-y.

[51] Fujii, K., Higuchi, K., and Rekimoto, J., "Endless flyer: A continuous flying drone with automatic battery replacement," *Proceedings - IEEE 10th International Conference on Ubiquitous Intelligence and Computing, UIC 2013 and IEEE 10th International Conference on Autonomic and Trusted Computing, ATC 2013*, 2013, pp. 216–223. doi:10.1109/UIC-ATC.2013.103.

[52] Sensefly, "User Manual eBee and eBee Ag," , 2014. URL http://95.110.228.56/documentUAV/dronemanual/%5BENG%5D_2014_Extended_User_Manual_eBee_and_eBee_Ag_v12_1.pdf.

[53] Vertical Technologies, "DeltaQuad Specifications," , 2017. URL https://www.verticaltechnologies.com/img/cms/DeltaQuadEUspecsV2.pdf.

[54] Sheu, J. B., "An emergency logistics distribution approach for quick response to urgent relief demand in disasters," *Transportation Research Part E: Logistics and Transportation Review*, Vol. 43, No. 6, 2007, pp. 687–709. doi:10.1016/j.tre.2006.04.004.

[55] Chang, F. S., Wu, J. S., Lee, C. N., and Shen, H. C., "Greedy-search-based multi-objective genetic algorithm for emergency logistics scheduling," *Expert Systems with Applications*, Vol. 41, No. 6, 2014, pp. 2947–2956. doi:10.1016/j.eswa.2013.10.026.

[56] Griva, I., Nash, S. G., and Sofer, A., *Linear and Nonlinear Optimization*, 2nd ed., Society for Industrial and Applied Mathematics, 2009.

[57] Weimin, D., "Chi-Chi, Taiwan Earthquake Event Report," Tech. rep., Risk Management Solutions, Menlo Park, CA, 2000. URL http://forms2.rms.com/rs/729-DJX-565/images/eq_chi_chi_taiwan_eq.pdf.

[58] Sheu, J. B., "Dynamic relief-demand management for emergency logistics operations under large-scale disasters," *Transportation Research Part E: Logistics and Transportation Review*, Vol. 46, No. 1, 2010, pp. 1–17. doi:10.1016/j.tre.2009.07.005.

[59] Ranquist, E., "Exploring the Range of Weather Impacts on UAS Operations," *18th Conference on Aviation, Range and Aerospace Meteorology*, American Meteorological Society, Seattle, WA, 2016, p. 11.

[60] Baronti, F., Fantechi, G., Fanucci, L., Leonardi, E., Roncella, R., Saletti, R., and Saponara, S., "State-of-charge estimation enhancing of lithium batteries through a temperature-dependent cell model," *International Conference on Applied Electronics (AE)*, Vol. 0, No. 1, 2011, pp. 1–5.

[61] SESAR, "European Drones Outlook Study," Tech. rep., SESAR, Brussels, Belgium, 2016. URL http://www.sesarju.eu/sites/default/files/documents/reports/European_Drones_Outlook_Study_2016.pdf.

[62] Emergency Telecommunications Cluster, "Humanitarian Unmanned Aerial Vehicles (UAV) Coordination Model," , 2017. URL https://www.etcluster.org/discussions/humanitarian-unmanned-aerial-vehicles-uav-coordination-model.